Computer Simulation of the Formation of Langmuir Solitons and Holes in a Cylindrical Magnetized Plasma Column

Turikov, V. A.

Publication date:
1978

Document Version
Publisher's PDF, also known as Version of record

Risø Report No. 380

Risø Report No. 380

Risø National Laboratory

Computer Simulation of the Formation of Langmuir Solitons and Holes in a Cylindrical Magnetized Plasma Column

by V. A. Turikov

June 1978

Sales distributors: Jul. Gjellerup, Sølvgade 87, DK-1307 Copenhagen K, Denmark

Available on exchange from: Risø Library, Risø National Laboratory, P.O. Box 49, DK-4000 Roskilde, Denmark

UDC 533.9 : 681.3 : 519.283

June 1978 Risø Report No. 380

Computer Simulation of the Formation of Langmuir Solitons and Holes in a Cylindrical Magnetized Plasma Column

by

V.A. Turikov*
Physics Department
Risø National Laboratory

*On leave from Patrice Lumumba University, Moscow W-302, USSR

Abstract

Nonlinear plasma ocsillations in a cylindrical plasma resulting from a short localized external excitation are examined by means of a particle-in-cell simulation scheme. Computer calculations are performed for describing the experimental results obtained in a single-ended Q-machine plasma in a cylindrical waveguide. We assume that there is a strong magnetic field in the direction of the column axis. When the amplitude of the excitation potential is close to the kinetic energy of electrons having a phase velocity of the electron plasma wave, the formation is observed of solitons and holes in phase space. After formation, the solitons and holes move with constant velocities. The velocities of solitons are close to the wave-phase velocity, while holes move with smaller velocities. When the external potential amplitude is increased, there is a tendency that the number of holes grows. The potential amplitude of the self-consistent field in the soliton region damps in time with increasing soliton width. The potential profile of the hole does not change after its formation.

ISBN 87-550-0536-5

ISSN 0418-6443

CONTENTS

1. INTRODUCTION

In this study nonlinear Langmuir oscillations in a collisionless plasma undergoing short localized excitation were investigated by means of the particle simulation method. The investigation was made in order to analyze the experiments in a single-ended Q-machine with a plasma in a cylindrical waveguide in a strong magnetic field[1]. The localized external excitation in these experiments was achieved by applying a short (about one electron plasma period) impulse of external potential in the space between the waveguide and a conducting cylinder of the same radius[2].

Electron plasma oscillations in a cylindrical plasma with a strong magnetic field have a dispersion relation[3] similar to that of ion-acoustic waves. Thus, under such conditions, it is possible to expect the formation of solitons[4,5] during excitations in the axial direction. In particular, electron plasma shock waves and solitons propagating in the Q-machine column have been observed experimentally[2,6]. It has been pointed out in the experiments of Saeki et al.[1] that with an excitation energy value close to the kinetic energy of electrons having the phase velocity of the plasma wave, holes occur in phase space in addition to solitons. These holes, which correspond to the positive humps of the electrostatic potential, move with constant velocities like solitons. After their formation, the holes apparently represent Bernstein-Green-Kruskal modes[7] which occur, for example, in the development of the two-stream instability[8].

Such a study is important for the investigation of the properties of a collisionless plasma of strong nonlinearity.

2. THE PHYSICAL PROBLEM

The numerical simulation presented here describes experiments with a Q-machine plasma in a cylindrical waveguide with a strong axial magnetic field. Space-charge waves can propagate in such a plasma in an axial direction. It is assumed that there is an infinite magnetic field so that the electrons are only able to move in the longitudinal direction (x-direction). The ions are assumed to form a stationary positive background.

The dispersion relation for the longitudinal Langmuir waves with phase velocities $\omega/k \ll c$ in such a plasma can be given the form[3]:

$$\omega^2 = \omega_{pe}^2 \frac{k^2}{k^2 + k_\perp^2} + \frac{3}{2}k^2 v_{th}^2 \qquad (1)$$

where $k_\perp = \frac{2.404}{r_o}$, r_o is a radius of plasma column, ω_{pe} is the electron plasma frequency, and v_{th} is the electron thermal velocity.

This dispersion relation takes into account only azimuthally symmetric modes of the electric field components.

Unlike the Langmuir oscillations in an infinite plasma, the oscillations described by the relation (1) have the maximum phase velocity for small wavenumbers $k \to 0$

$$v_{ph}^{max} = \frac{\omega_{pe}}{k_\perp} .$$

For the azimuthally symmetric modes, the electrostatic potential can be obtained from the Poisson equation

$$\frac{d^2\phi}{dx^2} - k_\perp^2\phi = -4\pi\rho . \qquad (2)$$

The term $-k_\perp^2\phi$ in eq. (2) describes the radial part of the Laplacian. Only one-dimensional electron movement is investigated and it is assumed that the charge density only varies in the x-direction too. It is clear that in a real plasma such an assumption is valid near the system axis. However, even with these limitations, we cannot neglect the term $\frac{1}{r}\frac{\partial}{\partial r}(rE_r)$ in the Poisson equation because the boundary condition on the waveguide surface $E_x(r=r_o) = 0$ must be fulfilled. As boundary conditions in x-space, we use the assumption of a zero electric field at the ends of the plasma column

$$\left.\frac{d\phi}{dx}\right|_{x=0} = \left.\frac{d\phi}{dx}\right|_{x=L} = 0 , \qquad (3)$$

where L is the column length.

The energy of the electric field described by eq. (2) can be calculated as

$$W_E = \frac{\pi r_o^2}{8\pi} \int (E_x^2 + k_\perp^2 \phi^2) dx \ . \qquad (4)$$

We suppose that the external potential that creates the localized excitation in the plasma between the cylinder and the waveguide can be presented in the form:

$$\phi_{ext}(x,t) = |\phi_{ext}|_{max} \cdot \eta(x) \cdot \sigma(t)$$

where $\eta(x), \sigma(t)$ are functions describing the space and time variations of the potential. In this study we use the following approximation:

$$\eta(x) = \begin{cases} -1 , & 0 \le x \le x_p - d_p , \\ -\frac{1}{2}\left[1+\cos\frac{\pi(x-x_p)}{d_p}\right] , & x_p - d_p \le x \le x_p , \\ 0 , & x_p < x \le L , \end{cases}$$

$$\sigma(t) = \begin{cases} \frac{1}{2}\left(1-\cos\frac{2\pi t}{\Delta t_p}\right) , & 0 \le t \le \Delta t_p , \\ 0 , & t > \Delta t_p , \end{cases}$$

where x_p, d_p and Δt_p are external potential parameters (see Fig. 1).

It is natural to choose the kinetic energy of the electron with phase velocity $v_{ph} = \omega_{pe}/k_\perp$ as a scale for the maximum value of the external potential

$$|\phi_{ext}|_{max} = A_p \cdot \frac{m_e}{2e} \left(\frac{\omega_{pe}}{k_\perp}\right)^2 = A_p \, W_{ph} \ ,$$

where parameters A_p defines the external potential in such a scale.

3. SIMULATION MODEL

In the present study the particle-in-cell method (PIC method) is employed for simulation of the nonlinear processes in

a plasma column under external excitation. The particle-in-cell method and related cloud-in-cell (CIC) method[8-11] have been used by many authors to investigate nonlinear phenomena in collisionless plasmas. Using the PIC method, Mason[12] investigated ion-acoustic shock waves. There the movement of the ions was simulated and the electrons were treated as a massless fluid. Because we are interested in electron Langmuir oscillations, we simulated the electron component and considered the ions as a positive stationary background.

In the particle-in-cell method it is convenient to use dimensionless variables defined by the following relations[13]:

$$X = \frac{x}{\Delta} , \quad V = v \cdot \frac{2\Delta t}{\Delta} ,$$

$$E = -E_x \frac{4(\Delta t)^2}{\Delta} \frac{e}{m_e} , \quad F = \phi \cdot \frac{2(\Delta t)^2}{\Delta^2} \frac{e}{m_e}$$

$$Q = -G \frac{\rho}{e n_o} , \quad G = 2\omega_{pe}^2 (\Delta t)^2 ,$$

where Δ is the space step, Δt is the time step, and n_o is the initial plasma density.

We use the leap frog scheme[13] for moving all simulation particles the time step $2\Delta t$:

$$V_m^{k+1} = V_m^{k-1} + E^k(X_m^k) + E_{ext}^k(X_m^k) , \tag{5}$$

$$X_m^{k+2} = X_m^k + V_m^{k+1} , \quad m = 1,2,\ldots N ,$$

where k is the number of the points at the time grid, N is the total number of simulation particles, and $E_{ext}(x)$ is the external electric field.

The first time step is realized by the Euler method[13]

$$X_m^1 = X_m^o + V_m^o/2 . \tag{6}$$

Having the co-ordinates of all particles at moment t^k, we can obtain the values of the charge density Q_i^k in the nodes of

the space grid. We calculate the charge density by distributing the charge of each particle between the two nearest grid points according to a reverse linear interpolation[8]. This method provides the reduction of shot noise inherent to the PIC model. Therefore we can express the values Q_i^k in the form:

$$Q_i^k = G[N_i(t^k)/N_c - 1] \ , \tag{7}$$

where $N_i(t^k)$ is the number of charges in e units in grid point i at time moment t^k, and N_c is the initial number of particles in each cell.

The value $N_i(t^k)$ is defined by reverse linear interpolation

$$N_i(t^k) = \sum_{m=1}^{N} \delta(\mathrm{Int}|X_m^k - i|)\cdot(1-|X_m^k - i|) \ , \tag{8}$$

where Int(z) is a truncation from real value to integer, and

$$\delta(m) = \begin{cases} 1 \ , & m = 0 \ , \\ 0 \ , & m \neq 0 \ . \end{cases}$$

It is easily shown that the charge distribution defined by eqs. (7) and (8) is equivalent to that in the cloud-in-cell method for homogeneous clouds with size Δ.

After calculating the charge density distribution Q_i^k, we can obtain new values of the self-consistent electric field in eqs. (5) for moving all particles the next time step. For this purpose, we have to solve the Poisson equation (2) with boundary conditions (3) using new charge density values. A simple three-point finite difference scheme is employed[13]

$$F_{i+1}^k - (2-k_i^2\Delta^2)F_i^k + F_{i-1}^k = Q_i^k \ . \tag{9}$$

The parabolic interpolation of potential values is used after solving eq. (9) to calculate the electric field E(x) in arbitrary points of the interval $0 \leq X \leq J$ ($J = L/\Delta$, see Appendix A1).

Equations (5)-(9) define the total time loop of the PIC method and are solved in each time step. The way in which the Poisson equation is solved is described in Appendix A2.

If a simulation particle is outside the interval $0 \leq X \leq J$ in some time step, the coordinate and the velocity of this particle are altered using reflecting boundary conditions,

$$x^k_{m,refl} = \begin{cases} -x^k_m , & x^k_m < 0 , \\ 2J - x^k_m , & x^k_m > J , \end{cases}$$

$$v^k_{m,refl} = - v^k_m .$$

We assume the initial distribution of the simulation particles is homogeneous in x-space and random in v-space according to the Maxwellian distribution

$$f_o(V) \sim \exp(- V^2/V^2_{th}) ,$$

where $V_{th} = v_{th} \cdot 2\Delta t/\Delta$.

The initial distribution in phase space and the velocity distribution obtained from it by a simple histogram is given in Fig. 2 ($N = 2 \cdot 10^4$).

The electric field energy (4) and the total plasma energy calculated per one particle are computed during the simulation process

$$W_E = \frac{1}{2GJ} \int_o^J [(E+E_{ext})^2 + 4k_1^2 \Delta^2 P^2] dX,$$
$$W_{total} = W_E + \frac{1}{N} \sum_{m=1}^{N} V^2_m . \qquad (10)$$

The procedure of calculating W_E is described in Appendix A1. The total energy calculation is used for checking the accuracy of the simulation method. It appeared during the computations that after $t > \Delta tp$, the total energy conserves with an error of about 1-2%. Such a conservation can be considered as a confirmation of a rather good accuracy of the model.

4. Computational Results and Discussion

The numerical computations were performed with typical parameters of the one-dimensional PIC simulation[8]. A space step Δ

was put equal to the Debye length λ_D and a time step was equal to $0.25/\omega_{pe}$ ($\simeq 0.04\ \tau_{pe}$, where τ_{pe} is a plasma period). The initial number of simulation particles in each cell N_c was equal to 50, with the total length of the space interval varying from 200 λ_D to 1000 λ_D, so the maximum number of particles used was $N = 5 \cdot 10^4$.

Runs were made with a radius of the plasma column of r_o = 20 λ_D and a length of the space interval between the cylinder and the wave guide (see Fig. 1) of d_p = 20 λ_D. These values correspond to the experimental parameters[1] for density, n_o = 10^7 cm^{-3}, and for thermal energy, E_o = 0.2 ev. As the right boundary value of the external potential jump (see Fig. 1), we used X_p = 410 λ_D for L = 800 λ_D and L = 1000 λ_D. The external impulse duration Δt_p was chosen equal to $2\tau_{pe}$.

Some of the computer simulation results are presented in Figs. 3-11. The plasma dispersion described by the relation (1) leads in a case of external excitation to the appearance of solitons moving with constant velocities in accordance with the theoretical treatments[4,5]. Soliton velocities are close to the phase velocity of space-charge waves $v_{ph} = \omega_{pe}/k_\perp$ for initial excitation energies of the order of W_{ph}. Increasing the external potential amplitude, increases the soliton velocities to the value 1.3 v_{ph} for A_p = 5.0 (see Fig. 9).

For potential amplitudes $e|\phi ext|_{max} \simeq W_{ph}$, the appearance of a hole in phase space was observed (Figs. 3,4). The hole moves with a constant velocity that is less than the soliton velocity. As shown in Fig. 9, its velocity also increases with A_p increasing up to a value of about 0.5 v_{ph}, changing the sign for some excitation amplitude.

For a larger potential jump amplitude ($A_p \gtrsim 3.0$), two holes appear in phase space (Figs. 5,6). With a further increase of the external excitation, there is a tendensy that the number of holes will increase (Figs. 7,8). They move with different velocities, moving behind the soliton and separated from each other.

From the potential space variations in equidistant time moments presented in Figs. 10, 11, some important facts can be derived. There are three regions, separated in space, of the disturbed potential arising from the different physical phenom-

ena. After their formation, all three regions move with constant but different velocities, moving away from each other.

The region on the right side with negative potential (positive in Figs. 10, 11 as we plotted - ϕ) represents a soliton moving approximately with a phase velocity v_{ph}. In the case $v_{ph} >> v_{th}$ (Fig. 10), this part of the disturbed potential has a fluid nature and can be described by the Korteveg-de Vries equation for Landmuir waves in cylindrical plasma[6]. In such conditions a soliton moves practically without damping. When v_{ph} is close to thermal velocity (Fig. 11), the interaction between waves and particles becomes stronger and soliton damping with increasing of its width takes place[14,15].

The left, non-stationary region of the positively disturbed potential is a region of electron deficit caused by the large amount of particles contributed to the soliton part. This positive pulse moves with a velocity close to v_{ph} and can also be described by the fluid model. Both of these fluid-type regions have a train of waves behind them with space-charge dispersion (1).

The central region of the potential disturbance is a stationary Bernstein-Green-Kruskal mode[7,8], being itself an esentially kinetic phenomenon caused by an electron distribution function disturbance under external field impulse.

Thus we can conclude that the simulation scheme used is good enough to describe the nonlinear Langmuir oscillations in a cylindrical plasma. The computer calculations confirmed the experimental results[1] of studying the formation of solitons and holes in a single-ended Q-machine under external excitation.

It would be of interest in future to investigate the more complicated effects of the interactions between holes and solitons for different external impulse profiles.

The simulation code was written in FORTRAN and run on a Burroughs 6700 at the Risø Computer Installation. A typical computing time for one time step and $N = 5 \cdot 10^4$ was about 15 sec.

ACKNOWLEDGEMENTS

This work was performed while the author was a visitor to the Risø National Laboratory. He is very grateful to V.O. Jensen for hospitality and for support of this work, as also to J.P. Lynov, P. Michelsen, H.L. Pécseli, J. Juul Rasmussen and K. Saeki for many helpful discussions.

References

1) K. Saeki, P. Michelsen, H. Pécseli, J. Juul Rasmussen, (to be published).

2) K. Saeki (1973), J. Phys. Soc. Japan, 35, 251-257.

3) A.W. Trivelpiece and R.W. Gould (1959), J. Appl. Phys. 30, 1784-93.

4) R.Z. Sagdeev (1966). Rev. Plasma Phys. 4, 65-91.

5) H. Washimi and T. Taniuti (1966), Phys. Rev. Letters, 17, 996-998.

6) H. Ikezi, P.J. Barret, R.B. White, and A.Y. Wong (1971), Phys. Fluids, 14, 1997-2005.

7) I.B. Bernstein, J.M. Green, and M.D. Kruskal, Phys. Rev. (1957) 108, 546-550.

8) R.L. Morse and C.W. Nielson (1969), Phys. Fluids, 12, 2418-2425.

9) R.W. Hockney (1966), Phys. Fluids, 9, 1826-35.

10) C.K. Birdsall and D. Fuss (1969), J. Comput. Phys., 3, 494-511.

11) R.L. Morse (1970), Methods Comput. Phys., 9, 213-39.

12) R.J. Mason (1971), Phys. Fluids, 14, 1943-58.

13) D. Potter (1973), Computational Physics (Wiley,London), 304 pp.

14) E. Ott and R.N. Sudan (1969), Phys. Fluids, 12, 2388-94.

15) E. Ott (1971), Phys. Fluids, 14, 748-750.

APPENDIX

A1. Electric Field and Energy Calculation

We calculate the potential values between the space grid nodes by means of the quadratic interpolation

$$F(X) = A_j X^2 + B_j X + C_j \ , \tag{11}$$

where index j is defined as j = Int(X) + 1, and A_i, B_i, C_i are the coefficients of the parabola crossing three points (i-1, F_{i-1}), (i, F_i), (i+1, F_{i+1}):

$$A_i = \frac{1}{2}(F_{i-1} - 2F_i + F_{i+1}) \ ,$$

$$B_i = F_{i+1} - F_i - A_i(2i+1) \ , \tag{12}$$

$$C_i = F_i - B_i \cdot i - A_i \cdot i^2 \ , \quad i = 1,2,\ldots,J-1.$$

For i = J, we assume

$$A_J = A_{J-1}, \quad B_J = B_{J-1}, \quad C_J = C_{J-1} \ .$$

We can obtain a value of the dimensionless electric field E(X) in an arbitrary point X from expression (11) by simple differentiation

$$E(X) = 2\,\frac{dF}{dX} = 2(2A_j X + B_j) \ .$$

For an electric field energy calculation, it is necessary to calculate two integrals

$$\int_0^J E^2 dX \ , \quad \int_0^J F^2 dX \ .$$

We can obtain the first by means of direct integration in each space step

$$\int_0^J E^2 dX = \sum_{i=1}^{J} \int_{i-1}^{i} E^2 dX = 4 \sum_{i=1}^{J} (4A_i^2 \frac{X^3}{3} + 2A_i B_i \frac{X^2}{2} + B_i^2 X) \Big|_{i-1}^{i} .$$

To calculate the second integral, we use parabolic interpolation for values F_i^2,

$$F^2(X) = \bar{A}_i X^2 + \bar{B}_i X + \bar{C}_i ,$$

where the coefficients $\bar{A}_i$, $\bar{B}_i$, $\bar{C}_i$ are defined by eqs. (12), replacing F_j by F_j^2. Therefore we can write

$$\int_0^J F^2(X) dX = \sum_{i=1}^{J} (\frac{\bar{A}_i}{3} X^3 + \frac{\bar{B}_i}{2} X^2 + \bar{C}_i X) \Big|_{i-1}^{i} .$$

A2. Solving of the Poisson Equation

The general boundary conditions for the Poisson equation (9) can be written in the form:

$$(A_\ell \frac{dF}{dX} + B_\ell F) \Big|_{X = 0} = C_\ell , \qquad (13)$$

$$(A_r \frac{dF}{dX} + B_r F) \Big|_{X = J} = C_r , \qquad (14)$$

where A_ℓ, B_ℓ, C_ℓ, A_r, B_r and C_r are prescribed constants.

For solving the Poisson equation (9) with boundary conditions (13), (14), we use the double recursive procedure[13] with the parabolic interpolation of potential for computing $\frac{dF}{dX}$ at the ends of the interval $0 \le X \le J$. The values of the potential in this procedure are defined by the recurrence formula:

$$F_j = c_j F_{j-1} + s_j , \quad j = 1,2,\ldots,J,$$

where the coefficients c_j and s_j are also defined by the recurrence relations:

$$c_{j-1} = \frac{1}{c_j - k_i^2\Delta^2 - 2} ,$$

$$s_{j-1} = \frac{Q_{j-1} - s_j}{c_j - k_i^2\Delta^2 - 2} , \quad j = J, J-1, \ldots, 2 .$$

The initial values c_J, s_J for these relations can be obtained from the boundary condition (14) for the right boundary of the interval

$$c_J = \frac{A_r + 1 - k_i^2\Delta^2/2}{A_r + B_r} ,$$

$$s_J = \frac{C_r - A_r Q_{J-1}/2}{A_r + B_r} . \qquad (15)$$

The value F_o can be found using the boundary condition (13) for the left boundary of the interval

$$F_o = \frac{C_\ell + A_\ell (c_2 s_1 - s_2 - 4s_1)/2}{A_\ell (2c_1 - c_1 c_2/2 - 3/2) + B_\ell} . \qquad (16)$$

Expressions (15) and (16) are obtained from eqs. (13) and (14) by means of quadratic interpolation of the potential values for calculating $\frac{dF}{dx}$.

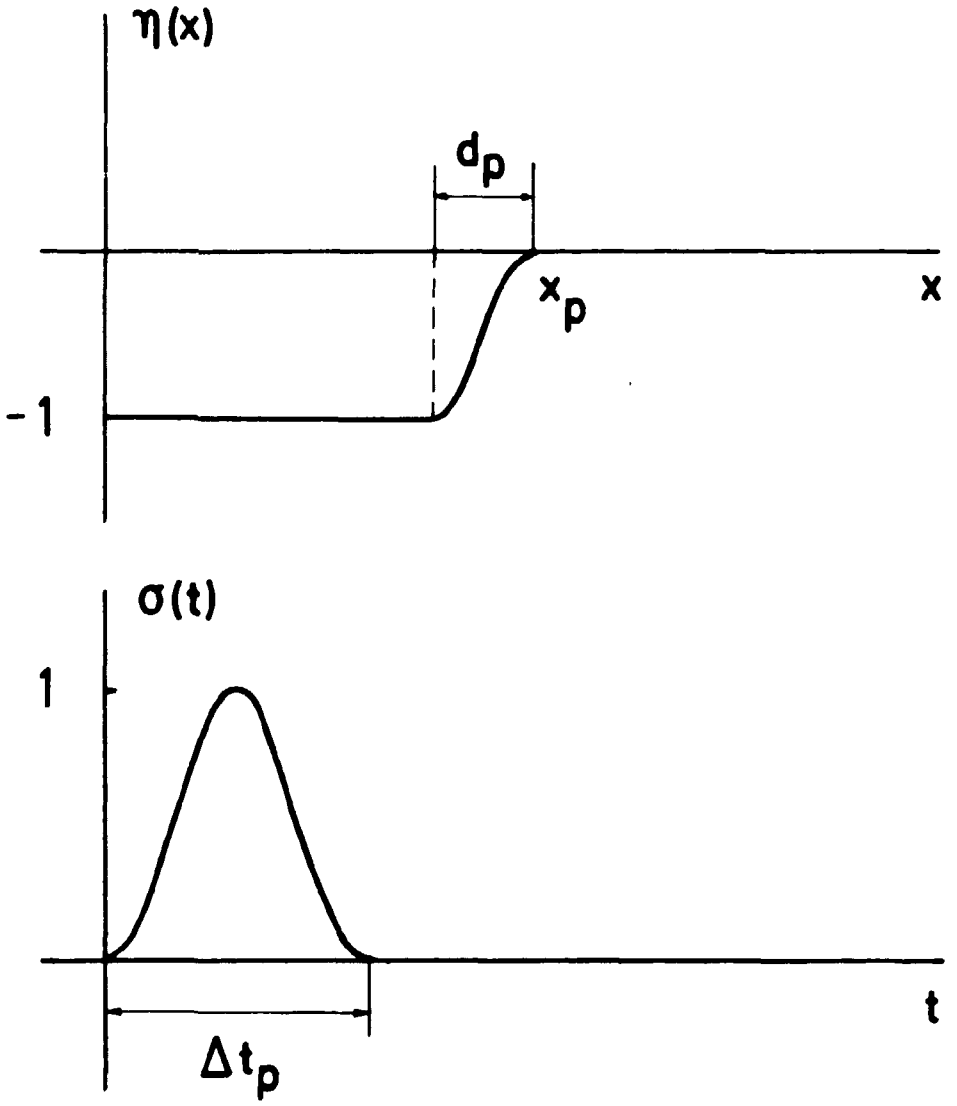

Fig. 1. Space and time variations of the excitation potential $e\phi_{ext} = A_p W_{ph} \eta(x) \sigma(t)$.

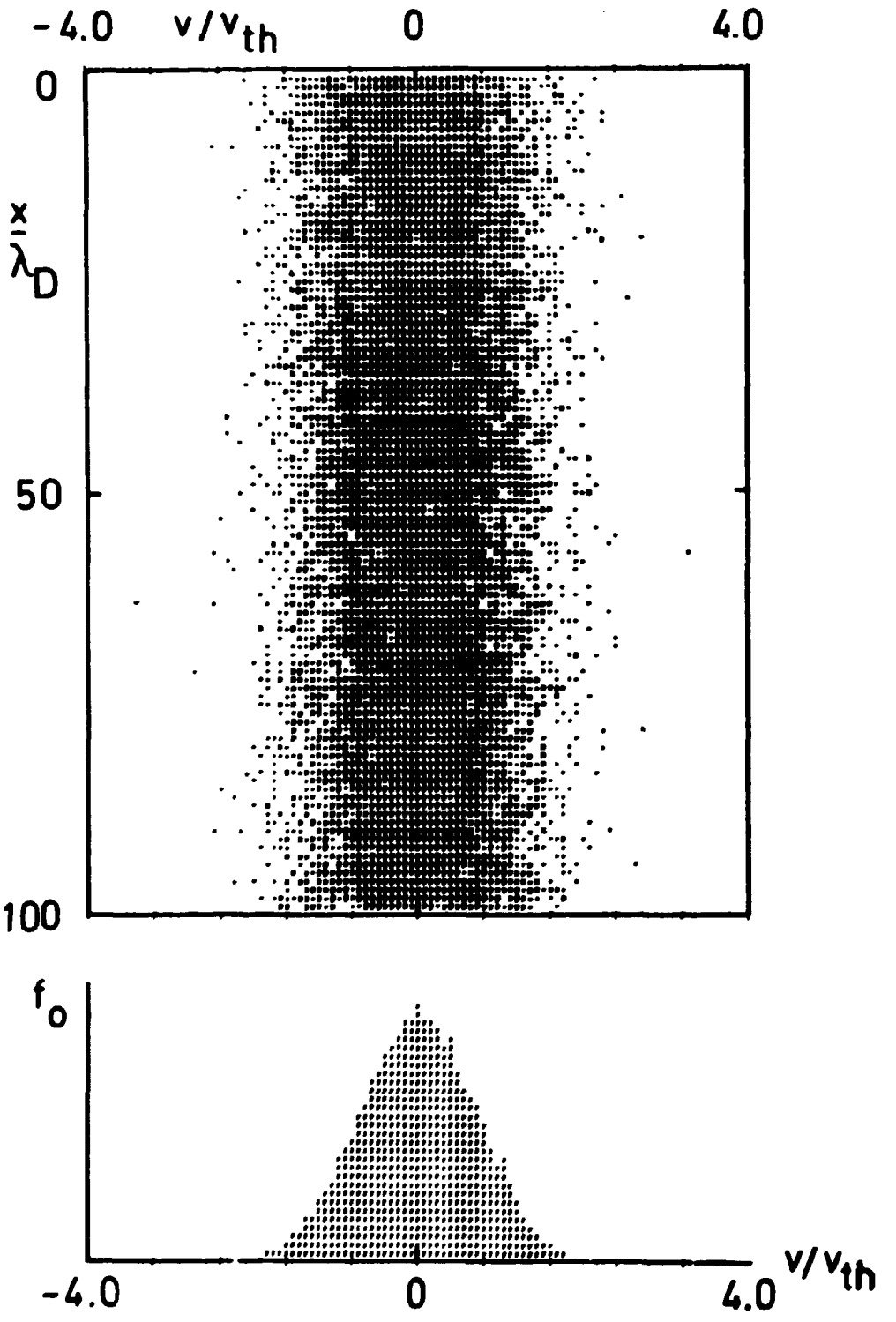

Fig. 2. Initial distribution of the simulation particles in phase space and in velocity space.

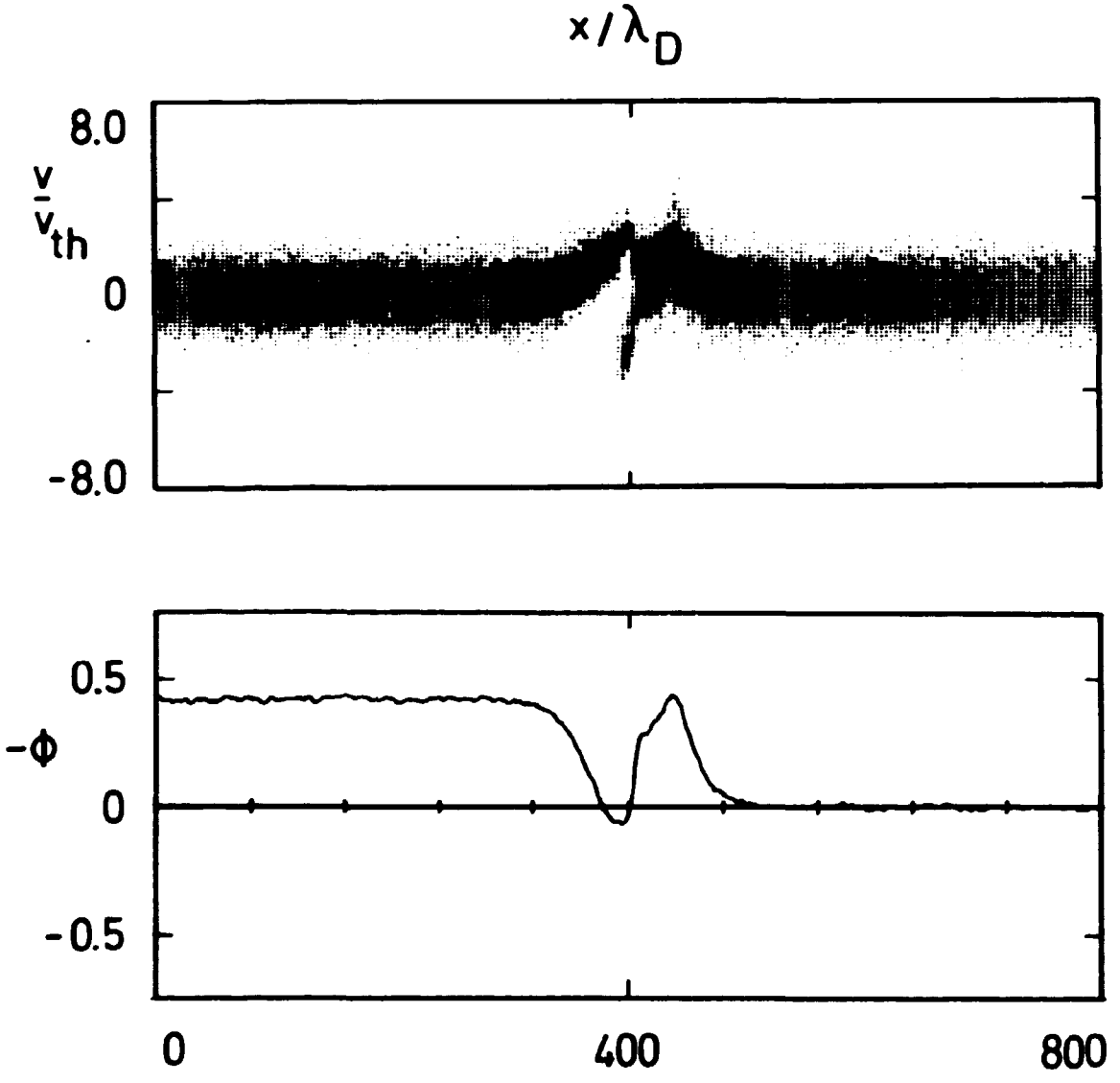

Fig. 3. Electron x,v-distribution and potential space variation for A_p = 1.0, t = 1.55 (in plasma periods). The potential is plotted in $A_p W_{ph}/e$ units.

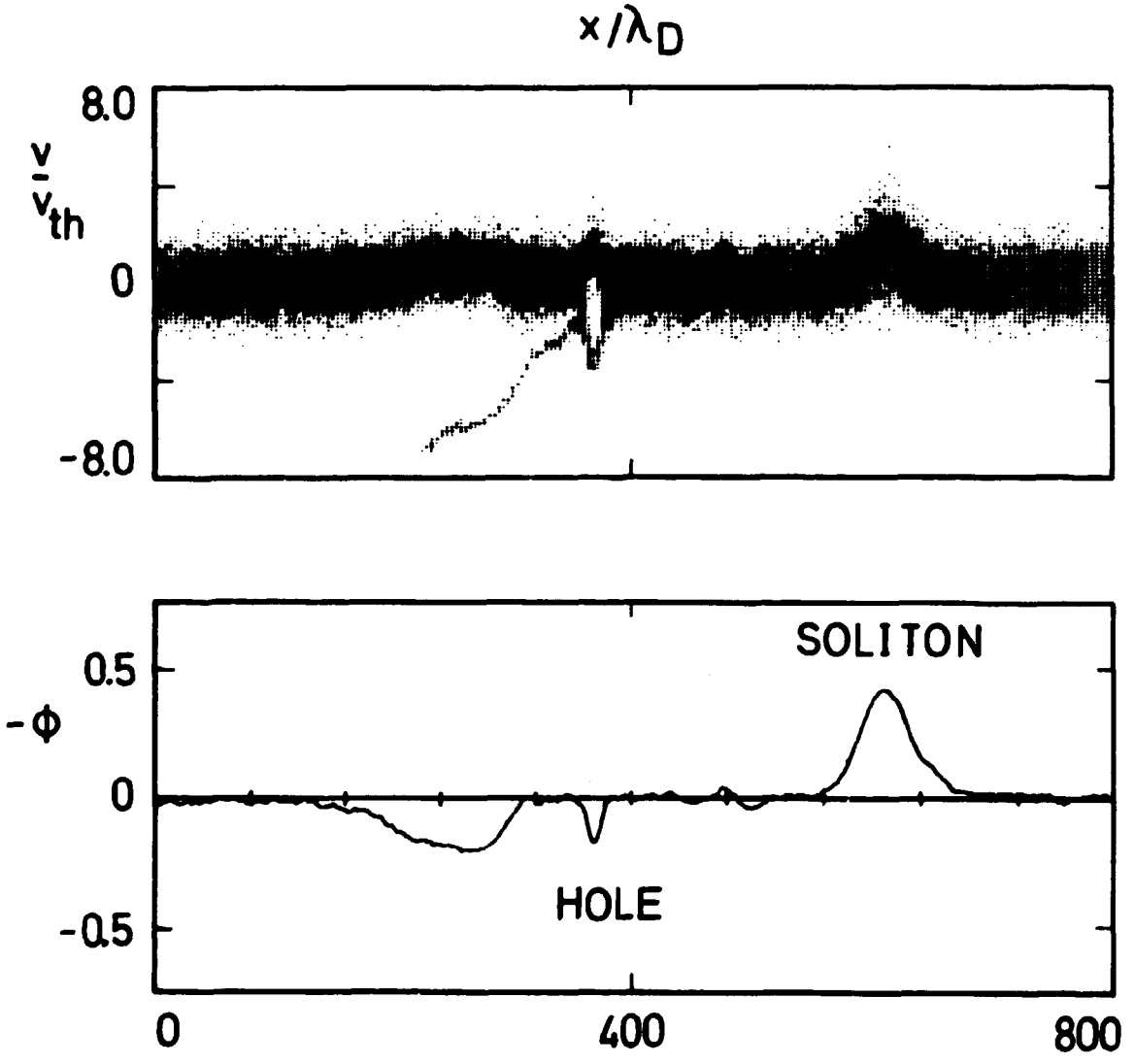

Fig. 4. $A_p = 1.0$, $t = 4.73$

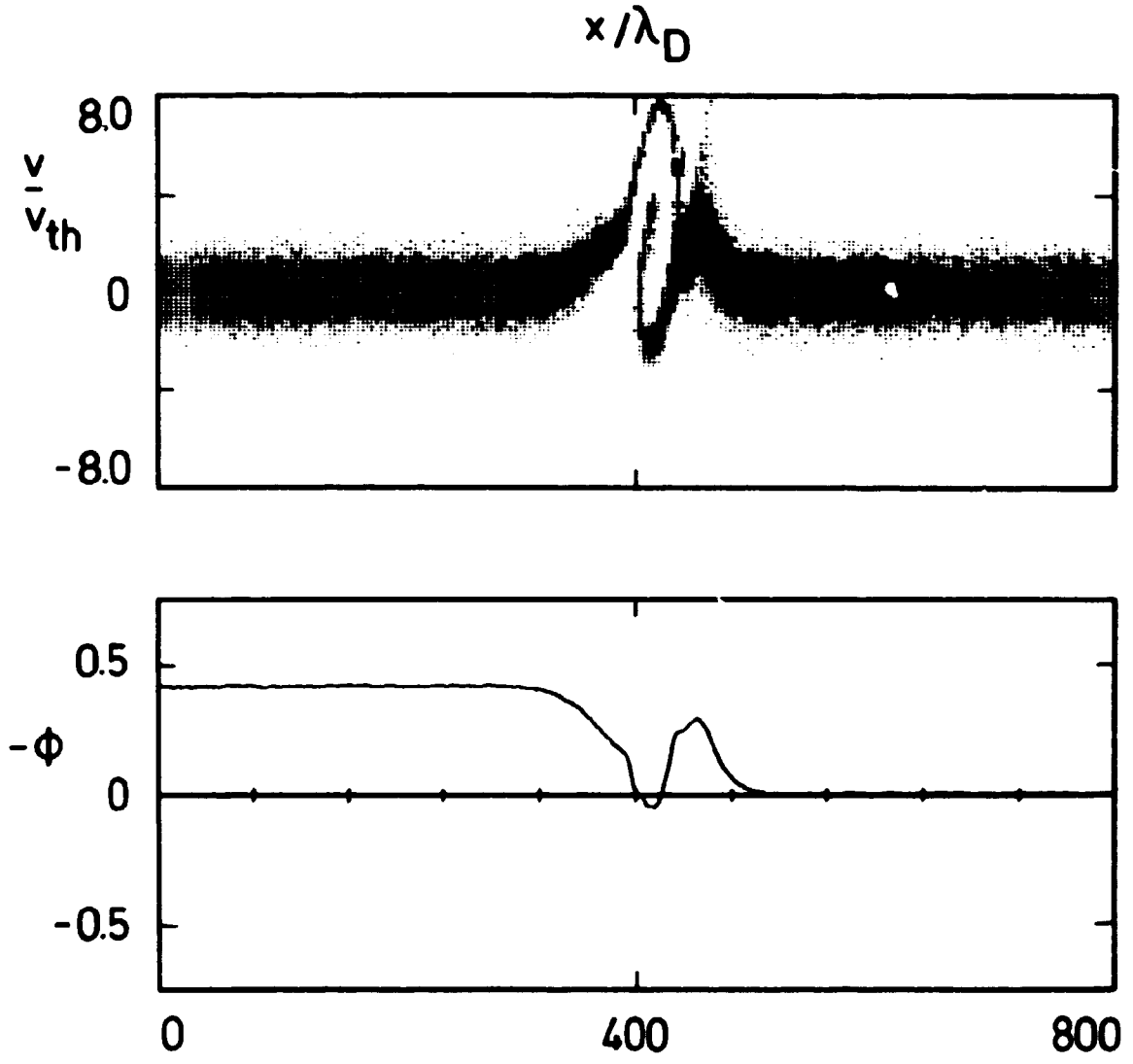

Fig. 5. $A_p = 3.0$, $t = 1.55$

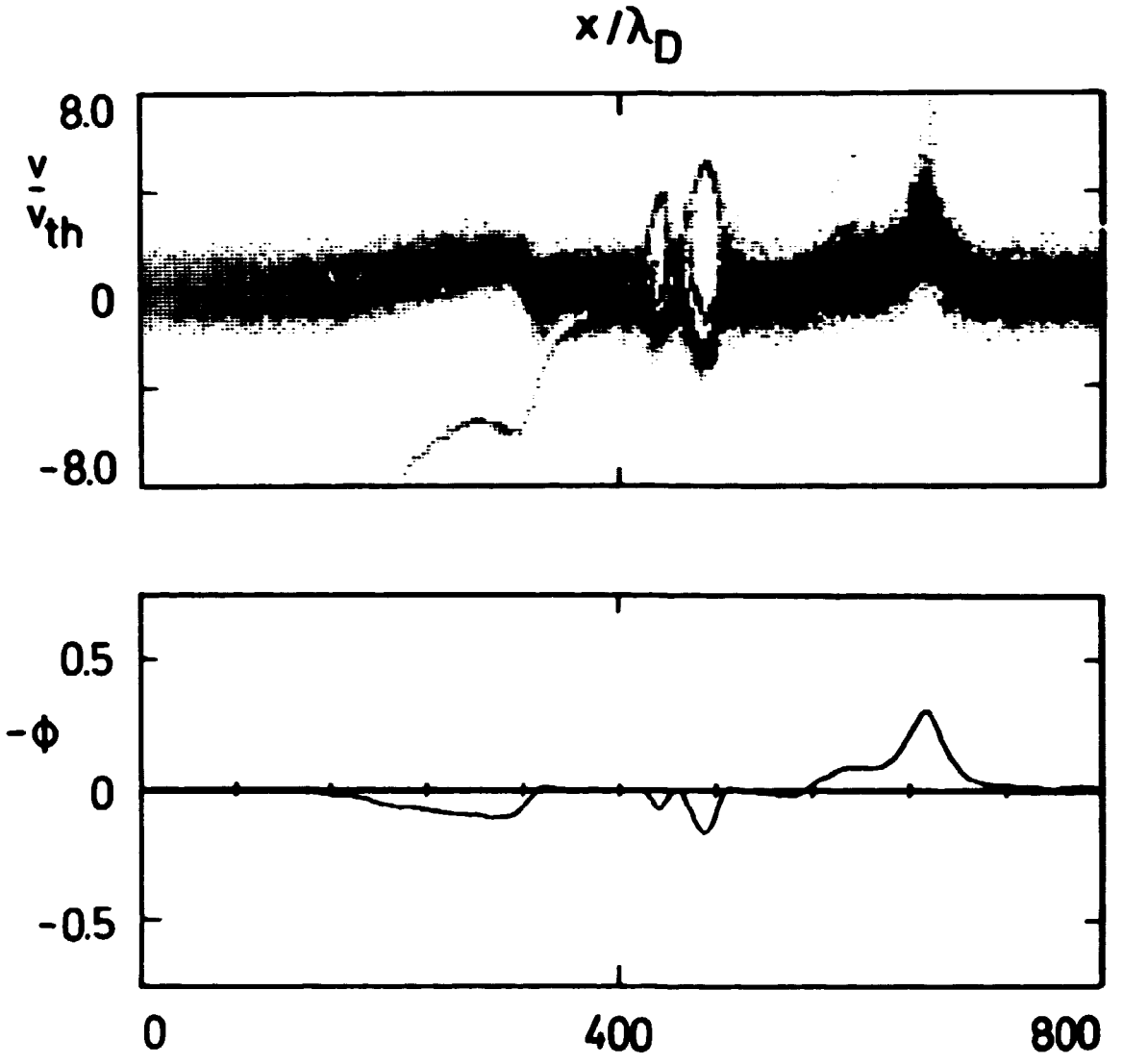

Fig. 6. $A_p = 3.0$, $t = 4.73$

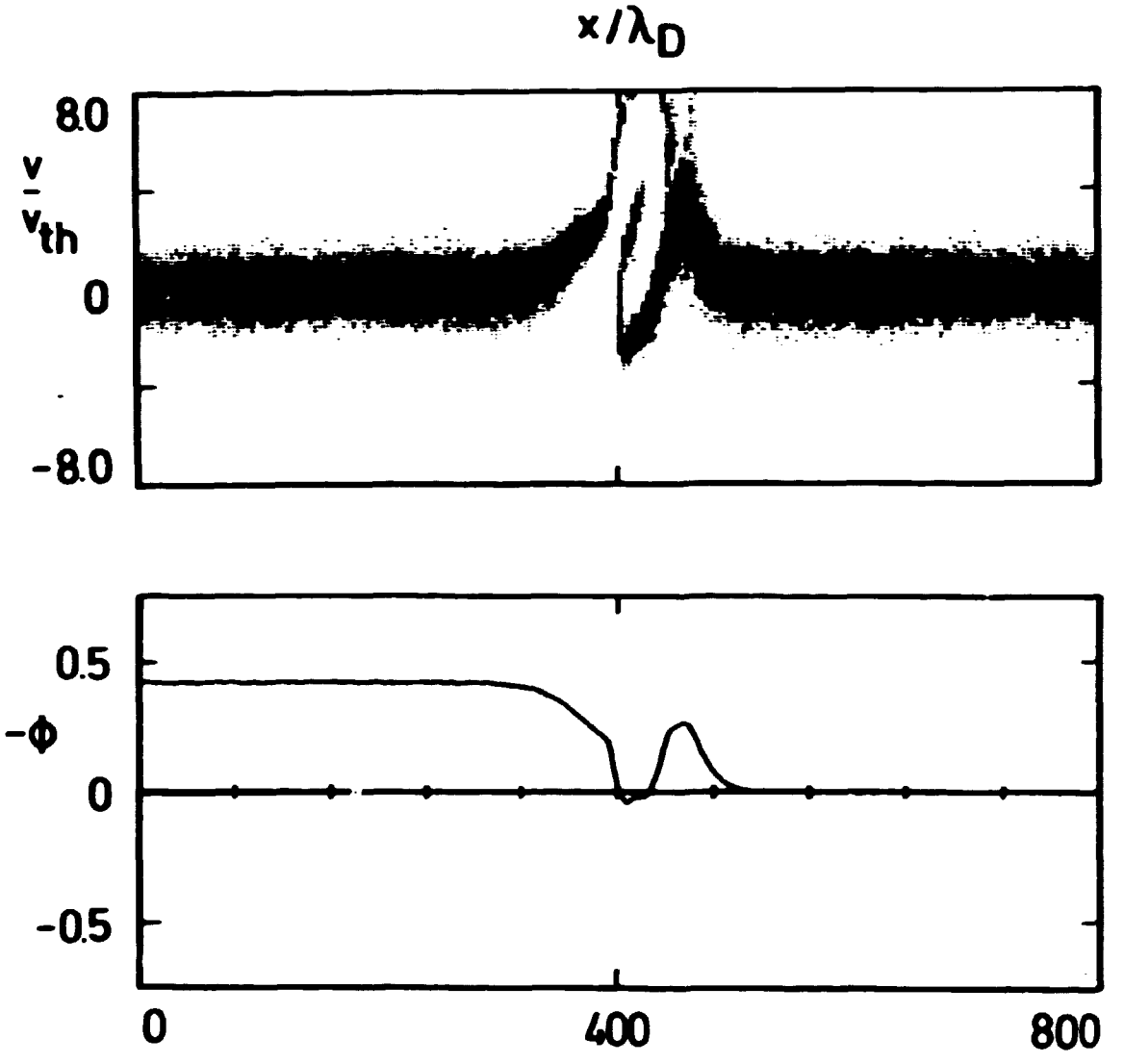

Fig. 7. $A_p = 4.0$, $t = 1.55$

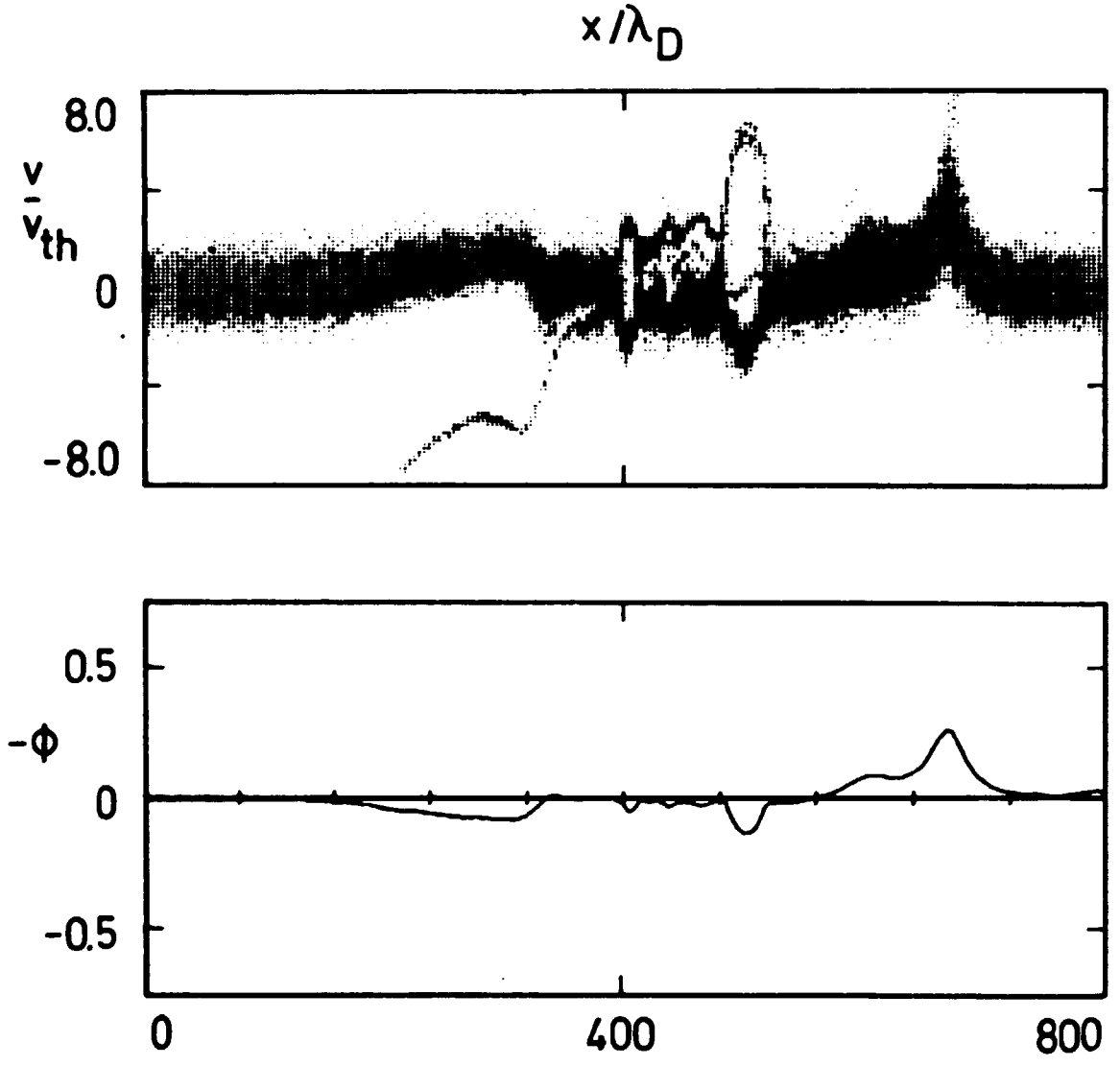

Fig. 8. $A_p = 4.0$, $t = 4.73$

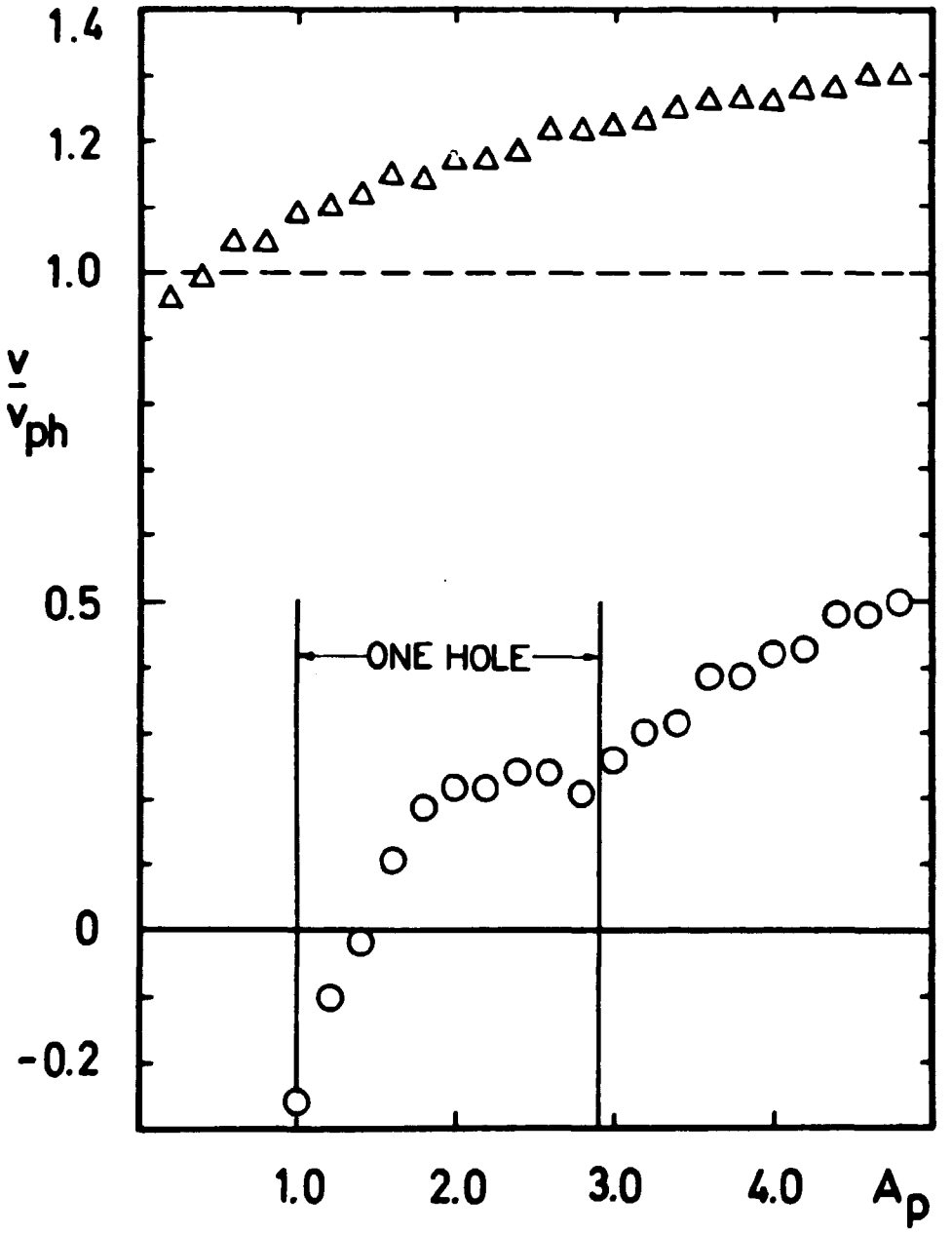

Fig. 9. Soliton (Δ) and hole (o) velocities in v_{ph} units versus the normalized potential amplitude A_p ($n_o = 10^7$ cm^{-3}, $E_o = 0.2$ ev). In the case of severel holes, the velocity of the fastest is shown.

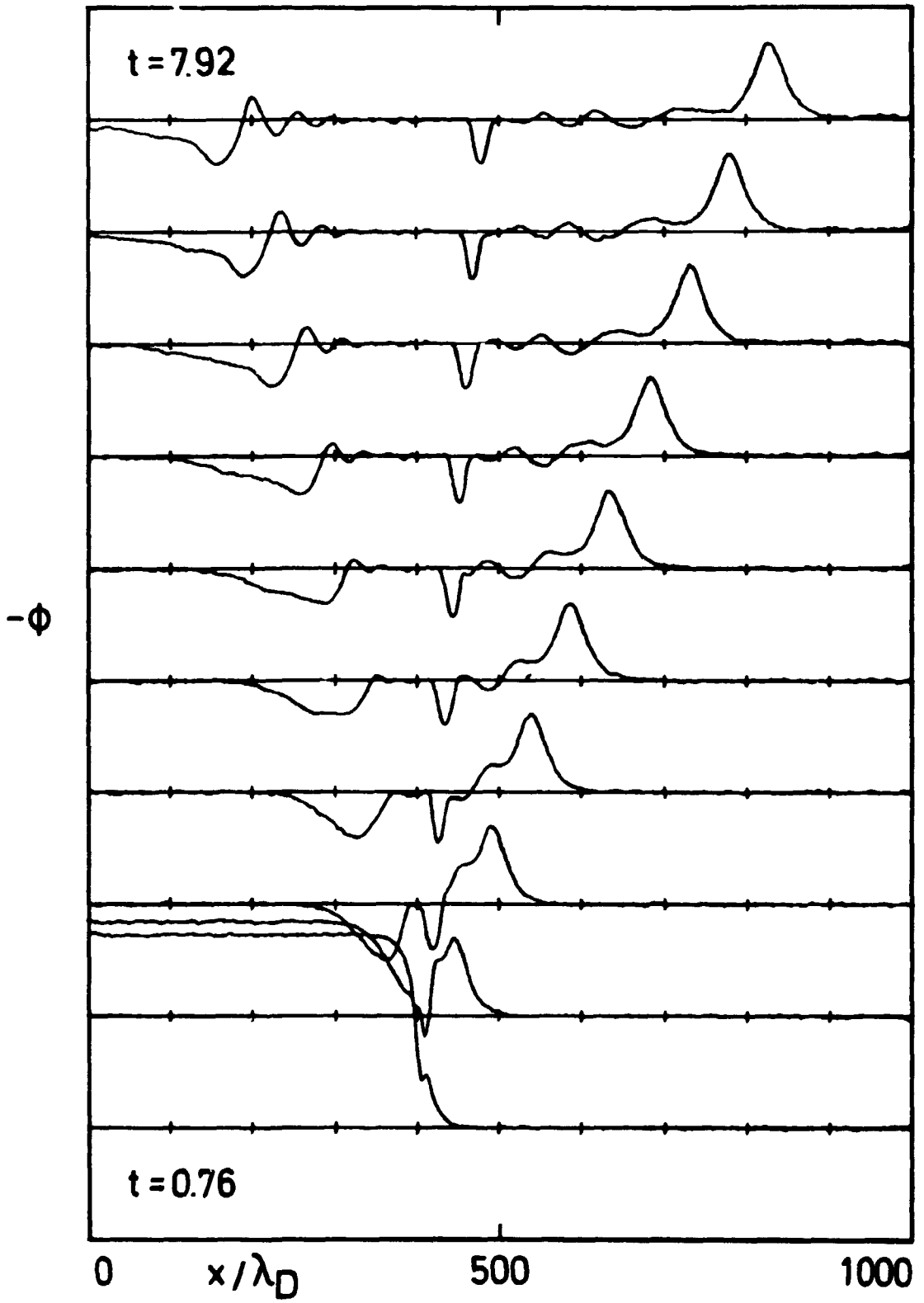

Fig. 10. Evolution of the potential for $A_p = 2.0$ ($n_o = 10^7$ cm^{-3}, $E_o = 2.0$ ev, $v_{ph} = 5.6\ v_{th}$). Time is expressed in plasma periods and each plot is drawn after 10 time steps ($\Delta t = 0.25/\omega_{pe}$).

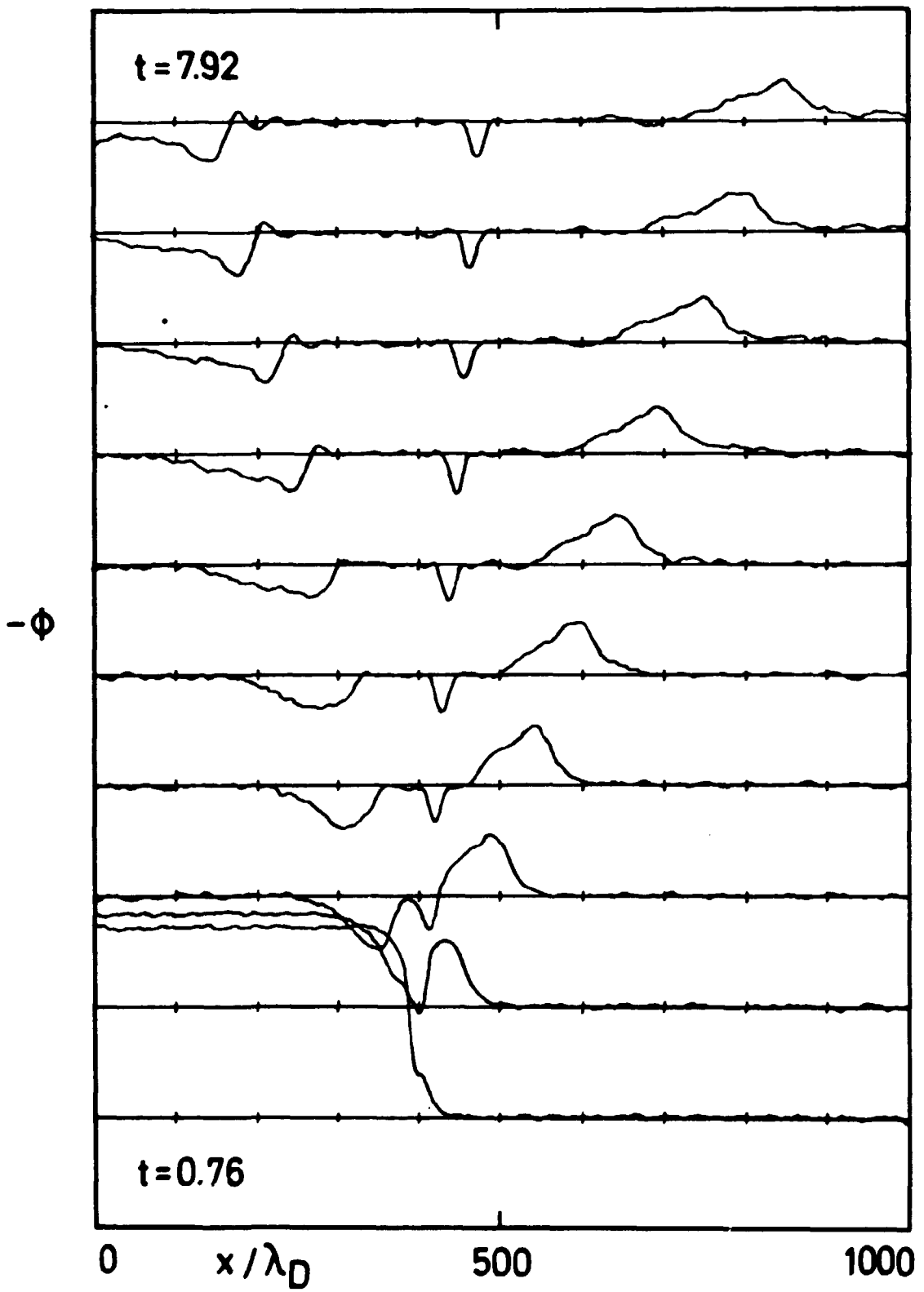

Fig. 11. Soliton damping for $v_{ph} = 2.8\ v_{th}$ ($n_o = 10^7\ cm^{-3}$, $E_o = 0.8$ ev).

ISBN 87-550-0536-5
ISSN 0418-6443